Hyperactivation of p21^{ras} and the Hematopoietic-specific Rho GTPase, Rac2, Cooperate to Alter the Proliferation of Neurofibromin-deficient Mast Cells In Vivo and In Vitro

David A. Ingram,[1,2] Kelly Hiatt,[3] Alastair J. King,[5] Lucy Fisher,[1,2] Rama Shivakumar,[1,2] Christina Derstine,[1,2] Mary Jo Wenning,[1,2] Bruce Diaz,[8] Jeffrey B. Travers,[4] Antoinette Hood,[4] Mark Marshall,[8] David A. Williams,[1,2,6,7] and D. Wade Clapp[1,2,3]

[1]*Herman B. Wells Center for Pediatric Research, and the* [2]*Department of Pediatrics, the* [3]*Department of Microbiology/Immunology, the* [4]*Department of Dermatology, the* [5]*Department of Medicine, and the* [6]*Department of Molecular Genetics, Indiana University School of Medicine, Indianapolis, IN 46202*
[7]*Howard Hughes Medical Institute, Indianapolis, IN 46202*
[8]*Eli Lilly and Company, Indianapolis, IN 46285*

Abstract

Mutations in the *NF1* tumor suppressor gene cause neurofibromatosis type I (NF1), a disease characterized by the formation of cutaneous neurofibromas infiltrated with a high density of degranulating mast cells. A hallmark of cell lines generated from NF1 patients or *Nf1*-deficient mice is their propensity to hyperproliferate. Neurofibromin, the protein encoded by NF1, negatively regulates p21^{ras} activity by accelerating the conversion of Ras-GTP to Ras-GDP. However, identification of alterations in specific p21^{ras} effector pathways that control proliferation in *NF1*-deficient cells is incomplete and critical for understanding disease pathogenesis. Recent studies have suggested that the proliferative effects of p21^{ras} may depend on signaling outputs from the small Rho GTPases, Rac and Rho, but the physiologic importance of these interactions in an animal disease model has not been established. Using a genetic intercross between *Nf1*$^{+/-}$ and *Rac2*$^{-/-}$ mice, we now provide genetic evidence to support a biochemical model where hyperactivation of the extracellular signal–regulated kinase (ERK) via the hematopoietic-specific Rho GTPase, Rac2, directly contributes to the hyperproliferation of *Nf1*-deficient mast cells in vitro and in vivo. Further, we demonstrate that Rac2 functions as mediator of cross-talk between phosphoinositide 3-kinase (PI-3K) and the classical p21^{ras}-Raf-Mek-ERK pathway to confer a distinct proliferative advantage to *Nf1*$^{+/-}$ mast cells. Thus, these studies identify Rac2 as a novel mediator of cross-talk between PI-3K and the p21^{ras}-ERK pathway which functions to alter the cellular phenotype of a cell lineage involved in the pathologic complications of a common genetic disease.

Key words: Rac • Pak • PI3-K • cross-talk • neurofibromatosis type 1

Introduction

Mutations in the *NF1* tumor suppressor gene cause neurofibromatosis type I (NF1),* a pandemic, autosomal dominant disorder with an incidence of 1 in 3,000. Neurofibromin, the protein encoded by *NF1*, functions as a GTPase-activating protein (GAP) for p21^{ras} by accelerating the conversion of active p21^{ras}-GTP to inactive p21^{ras}-GDP (1, 2). Cutaneous neurofibromas are slow-growing tumors that are pathognomonic for NF1, and mast cells have been implicated in the pathogenesis of neurofibroma formation as well as other cutaneous tumors (3–7). Recently, we have

A. King's current address is SmithKline Beecham Pharmaceuticals, P.O. Box 1539, King of Prussia, PA 19406.

Address correspondence to D. Wade Clapp, Cancer Research Institute, 1044 W. Walnut, Rm. 408, Indianapolis, IN 46202. Phone: 317-274-4719; Fax: 317-274-8679; E-mail: dclapp@iupui.edu

**Abbreviations used in this paper:* BMMC, bone marrow–derived mast cell; ERK, extracellular signal–regulated kinase; GAP, GTPase-activating protein; MKP, mitogen-activated protein kinase phosphatase; NF1, neurofibromatosis type I; PI-3K, phosphoinositide 3-kinase; rmSCF, recombinant murine SCF; SCF, stem cell factor.

shown that $Nf1^{+/-}$ mice have increased numbers of peritoneal mast cells compared with wild-type littermates (8). In addition, bone marrow–derived mast cells (BMMCs) cultured from $Nf1^{+/-}$ mice demonstrate increased proliferation relative to wild-type cells in response to stem cell factor (SCF), a known mitogen for mast cells (8). However, although these studies show that alterations in $p21^{ras}$ activity can alter mast cell fates in vitro and in vivo, little is known about the contribution of specific $p21^{ras}$ effector pathways to the hyperproliferation of $Nf1^{+/-}$ mast cells or other *Nf1*-deficient cell types.

Although a critical role for $p21^{ras}$ in controlling cellular proliferation has been clearly established, recent studies have focused on identifying specific $p21^{ras}$ effector pathways important for cell cycle progression. Several studies have suggested that the proliferative effects of $p21^{ras}$ may depend on signaling inputs from the small Rho GTPases, Rac and Rho (9). Like $p21^{ras}$, the small Rho GTPases exist in an inactive (GDP-bound) and active (GTP-bound) conformation, and interact with target proteins in their GTP-bound state (9). However, although these studies have implicated cross-talk between $p21^{ras}$ and the Rho GTPases in controlling cellular proliferation, the mechanisms underlying these interactions are still relatively poorly defined (9). In addition, the physiological importance of signaling mechanisms that link $p21^{ras}$ and the Rho GTPases and its contribution to disease pathogenesis have not been established.

Previous studies have emphasized that loss of neurofibromin results in hyperactivation of the classical $p21^{ras}$-Raf-Mek-extracellular signal–regulated kinase (ERK) signaling pathway in *Nf1*-deficient cells leading to hyperproliferation (10, 11). However, the contribution of Rho GTPases to this signaling cascade and to the *Nf1* cellular phenotype have not been previously investigated in primary cells and in an animal disease model. Using $Nf1^{+/-}$ mice and BMMCs, we now provide pharmacologic, genetic, and biochemical data to support a model where hyperactivation of ERK mediated through the hematopoietic-specific Rho GTPase, Rac 2, directly contributes to the hyperproliferation of *Nf1*-deficient mast cells in vitro and in vivo. In addition, we demonstrate that ERK activation in response to SCF in mast cells is dependent on cross-cascade signals from phosphoinositide 3-kinase (PI-3K) converging on the $p21^{ras}$-Raf-Mek-ERK pathway. Importantly, we identify Rac2 as a novel mediator of cross-talk between these two pathways and provide evidence that hyperactivation of Rac2 can cooperate with $p21^{ras}$ to alter the function of a cell lineage implicated in the pathogenesis of a common genetic disease.

Materials and Methods

Animals. $Nf1^{+/-}$ mice were obtained from Tyler Jacks at the Massachusetts Institute of Technology (Cambridge, MA) in a C57BL/6.129 background and backcrossed for 13 generations into the C57BL/6J strain. $Rac2^{-/-}$ mice were backcrossed into a C57BL/6J as described previously (12). These studies were conducted with a protocol approved by the Indiana University Laboratory Animal Research Center. The *Nf1* and *Rac2* allele were genotyped as described previously (12–14). Multiple F0 founders were used to generate the four *Nf1* and *Rac2* genotypes used in these experiments as outlined. F0: $Nf1^{+/-}$; +/+ × +/+; $Rac2^{-/-}$. F1: $Nf1^{+/-}$; $Rac2^{+/-}$ × +/+; $Rac2^{+/-}$. F2: $Nf1^{+/-}$; $Rac2^{-/-}$, +/+; $Rac2^{-/-}$, $Nf1^{+/-}$; +/+, +/+; +/+.

Bone Marrow Mast Cell Culture and Proliferation Assays. Six to nine BMMCs from each murine genotype were generated and used for proliferation and biochemistry assays. All experiments were conducted using at least three lines from each genotype. BMMCs were cultured as described previously (15) with minor modifications and homogeneity of BMMCs was determined by Giemsa staining. Aliquots of cells were also stained with alcian blue and safranin to confirm that they were mast cells. Furthermore, FACS® analysis revealed similar forward and side light scatter characteristics and the same percentage of c-kit$^+$ expression in BMMCs of all murine genotypes (data not shown). Proliferation assays were performed as described previously (8). BMMCs from each genotype were deprived of growth factors for 24 h, and 3×10^5 cells were plated in 24-well dishes in 1 ml RPMI containing 1% glutamine (BioWhittaker), 1.5% HEPES (BioWhittaker), 2% penicillin/streptomycin (BioWhittaker), and 25–100 ng/ml recombinant murine SCF (rmSCF; PeproTech) or no growth factors as indicated in a 37°C, 5% CO_2, humidified incubator. In some experiments, LY294002 (Sigma-Aldrich), PD98059 (New England Biolabs, Inc.), or DMSO (Sigma-Aldrich) was added to the cultures 15 min to 1 h before addition of rmSCF. After 72 h, cells were counted using a hemocytometer. Cell viability was determined by a trypan blue exclusion assay. Assays were performed in triplicate.

For thymidine incorporation assays, BMMCs were deprived of growth factors for 24 h and 10^5 cells were plated in 96-well dishes in 200 ml of RPMI containing 1% glutamine, 10% fetal bovine serum (Hyclone Laboratories), and 25–100 ng/ml of rmSCF or no growth factors, as indicated, in a 37°C, 5% CO_2, humidified incubator. Cells were cultured for 48 h, and tritiated thymidine (New Life Science Products, Inc.) was added to cultures 6 h before harvest. In some experiments, LY294002, PD98059, or DMSO was added to the cultures 15 min to 1 h before addition of rmSCF. Cells were harvested on glass fiber filters (Packard Instrument Co.) and β emission was measured. Assays were performed in triplicate.

Raf-1, Mek, ERK, Pak1, and Akt In Vitro Kinase Assays. Activation of Raf-1, Mek, ERK, Pak1, and Akt kinases was determined by depriving BMMCs of serum and growth factors for 18–24 h and followed by stimulation with 10–100 ng/ml rmSCF for various amounts of time. Cells were washed twice with PBS containing 1 mM sodium orthovanadate and lysed in nonionic lysis buffer (20 mM Tris/HCl, 137 mM NaCl, 1 mM EGTA, 1% Triton X-100, 10% glycerol, 1.5 mM $MgCl_2$, and complete protease inhibitors (Amersham Pharmacia Biotech), as described previously (16). The protein lysates were equalized for protein concentration using the bicinchoninic acid (BCA) assay (Pierce Chemical Co.), and equal loading of protein in these assays was confirmed by Western blot. ERK and Pak1 kinase immunoprecipitations were carried out with an anti-ERK-2 (C-14) antibody (Santa Cruz Biotechnology, Inc.) and an anti-Pak1(C-19) antibody (Santa Cruz Biotechnology, Inc.), respectively. Raf-1 and Mek kinase immunoprecipitations were carried out with an anti-Raf-1 (C-12) antibody (Santa Cruz Biotechnology, Inc.) and an anti-Mek-1 (C-18) antibody (Santa Cruz Biotechnology, Inc.), respectively. Akt kinase immunoprecipitations were carried out

with an anti-Akt antibody (Cell Signaling Technology). The kinase immune complex assay was performed as described previously (16) and the following proteins were used as phosphorylation substrates: Elk-1 fusion protein (New England Biolabs, Inc.) for ERK kinase, histone 2B (Roche) for Akt kinase, myelin basic protein (Sigma-Aldrich) for Pak1 kinase, and recombinant Mek1 fused with GST at the NH_2 terminus (Upstate Biotechnology) for Raf-1 kinase. For Mek, Raf-1, and ERK, kinase reactions were resolved on 10% Tris-glycine gels (Novex). For Pak1 and Akt, kinase reactions were resolved on 4–20% gradient Tris-glycine gels (Novex), and transferred to polyvinylidine difluoride (PVDF) filters. Gels and PVDF filters were dried and subjected to autoradiography. Densitometry of individual bands was conducted using NIH Image software.

Ras and Rac Activation Assays. BMMCs were deprived of serum and growth factors for 18–24 h and stimulated at various amounts of time with 10–100 ng/ml rmSCF. Ras and Rac activation was subsequently determined using Ras and Rac activation assay kits (Upstate Biotechnology) according to the manufacturer's protocol and as described previously (17).

Immunoprecipitation and Western Blotting. BMMCs were lysed in nonionic lysis buffer as described previously (16). Cleared lysates were normalized for protein content using the BCA assay (Pierce Chemical Co.) and proteins were immunoprecipitated with protein A sepharose beads (Amersham Pharmacia Biotech) coupled with polyclonal antibodies for Raf-1 and Mek (Santa Cruz Biotechnology, Inc.). Immunoprecipitates were washed three times in lysis buffer, resuspended in sample buffer, boiled for 5 min, subjected to SDS-PAGE, and transferred to nitrocellulose. The membranes were blocked in TBS-Tween containing 5% BSA overnight. Membranes were incubated for 1–3 h at room temperature with the following antibodies: anti-phospho-Mek 1/2 (1:1,000; New England Biolabs, Inc.), anti-phospho-Raf-1 338 (1:5,000; Upstate Biotechnology), anti-phospho-Mek 298 (gift from Dr. M. Marshall), and anti-$p21^{ras}$ (Upstate Biotechnology). Secondary antibodies used were either anti–rat, anti–rabbit, or anti–mouse Ig horseradish peroxidase conjugated (Transduction Laboratories). Proteins were visualized by enhanced chemiluminescence (Santa Cruz Biotechnology, Inc.).

Studies In Vivo. Adult $Nf1^{+/-}$, $+/+Rac2^{-/-}$, $Nf1^{+/-}Rac2^{-/-}$, and wild-type mice received a continuous infusion of various doses of rmSCF or vehicle (PBS) from microosmotic pumps (Alzet) placed under the dorsal back skin. Osmotic pumps were surgically placed under light avertin anesthesia. rmSCF or vehicle was released over 7 d at a rate of 0.5 μl/hour, and osmotic pumps were surgically removed on day 7 after sacrifice by cervical dislocation. To accurately identify cutaneous sections for quantitating changes in mast cell numbers in response to rmSCF, the dorsal skin was stained with a drop of India ink at the point of exit of rmSCF from the osmotic pump before removal of the pump. 3-cm sections of skin marked with India ink were removed, fixed in buffered formalin, and processed in paraffin-embedded sections. Specimens were stained with hematoxylin and eosin to assess routine histology and with Giemsa to identify mast cells. Cutaneous mast cells were quantitated in a blinded fashion by counting 2-mm^2 sections in proximity to the India ink stain.

For studies evaluating basal numbers of mast cells in the *Nf1* and *Rac* intercrossed genotypes, 1-cm sections of ears were removed, fixed in buffered formalin, and processed in paraffin-embedded sections. Specimens were stained with hematoxylin and eosin to assess routine histology and Giemsa to identify mast cells. Cutaneous mast cells from four to five mice per experimental group were quantitated.

Results

$Nf1^{+/-}$ Mast Cells Have Increased $p21^{ras}$ Activity and Hyperactivation of Akt after Stimulation with SCF. SCF binding to its receptor, c-kit, causes a rapid increase in $p21^{ras}$ activity in primary BMMCs, and neurofibromin functions as a GAP for $p21^{ras}$ (1, 2, 15). However, it remains unclear whether heterozygosity of *Nf1* alters $p21^{ras}$ activity in primary cells. To investigate whether heterozygosity at the *Nf1* allele alters $p21^{ras}$ activity in mast cells, $Nf1^{+/-}$ and wild-type BMMCs were stimulated with SCF and assayed for changes in active $p21^{ras}$-GTP levels. After stimulation of BMMCs, levels of GTP-bound $p21^{ras}$ in cellular lysates were determined by precipitating the active GTPase with a GST fusion of the $p21^{ras}$ binding domain of Raf-1 kinase in an effector pull-down assay. Even though $Nf1^{+/-}$ mast cells had detectable, but reduced, levels of neurofibromin as determined by Western blot (data not shown), $Nf1^{+/-}$ mast cells had higher basal and SCF-stimulated $p21^{ras}$-GTP levels compared with wild-type cells (Fig. 1 A). Importantly, preincubation of both mast cell genotypes with PI-3K inhibitors, wortmannin or LY294002, did not alter $p21^{ras}$ activity (data not shown). Thus, these data position $p21^{ras}$ either in parallel or upstream of PI-3K in mast cells and demonstrate that heterozygosity at *Nf1* alters $p21^{ras}$ activity in primary BMMCs.

Direct binding of the activated c-kit receptor tyrosine kinase to the SH2 domain of the p85α regulatory subunit of type I_A PI-3K is important for kinase activation after stimulation by its ligand, SCF (15). Importantly, in immortalized cell lines $p21^{ras}$-GTP has previously been shown to bind to specific p110 catalytic subunits of type I_A PI-3K to augment kinase activity (18–20). To determine the effect of increased $p21^{ras}$-GTP levels on PI-3K activity in $Nf1^{+/-}$ mast cells, we compared the activation of the serine/threonine protein kinase B (PKB), also known as Akt, in $Nf1^{+/-}$ and wild-type BMMCs after stimulation with SCF. Activation of Akt is PI-3K dependent and provides a sensitive measure for PI-3K activity (21). $Nf1^{+/-}$ BMMCs demonstrated greater basal and SCF-stimulated Akt activity compared with wild-type cells over a range of SCF concentrations from 10 ng/ml (Fig. 1 B) to 100 ng/ml (data not shown). In addition, inhibitors of PI-3K inhibited Akt activity in both mast cell genotypes (Fig. 1 B), confirming that $p21^{ras}$ contribution to Akt activation is dependent on activation of PI-3K. Taken together, these data demonstrate that increased $p21^{ras}$ activity in $Nf1^{+/-}$ BMMCs after SCF stimulation is biochemically linked to increased activation of the PI-3K-Akt kinase pathway.

Hyperproliferation of $Nf1^{+/-}$ Mast Cells in Response to SCF Is Mediated through Cross-Cascade Activation of ERK from PI-3K. Proliferation of wild-type BMMCs in response to SCF is dependent on PI-3K activation (15). Although we have previously shown that $Nf1^{+/-}$ mast cells have increased proliferation in response to SCF, identification of $p21^{ras}$ effector pathways responsible for this phenotype remain unclear. To test whether SCF-induced hyperproliferation of $Nf1^{+/-}$ BMMCs is mediated through hyperactiva-

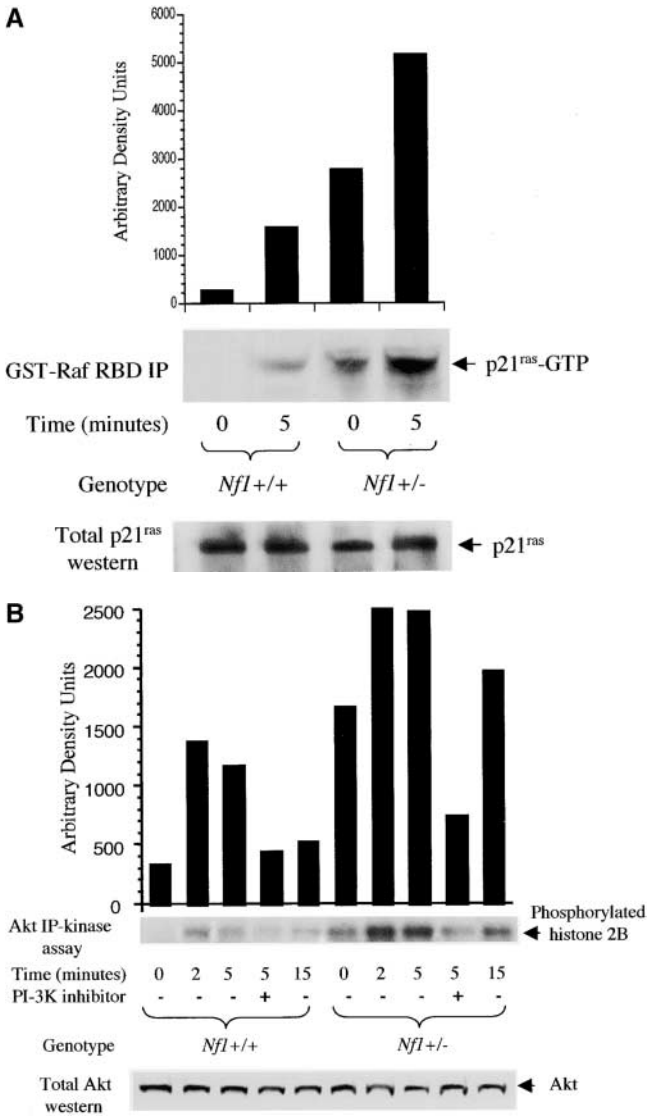

Figure 1. Analysis of $p21^{ras}$ activity and Akt kinase activity of $Nf1^{+/-}$ and wild-type BMMCs stimulated with SCF. (A) $p21^{ras}$ activity in $Nf1^{+/-}$ and wild-type BMMCs. GTP-bound $p21^{ras}$ levels were determined by incubating cell lysates with Raf-1 $p21^{ras}$ binding domain (RBD) agarose beads, fractionating immunoprecipitations by SDS-PAGE, and probing with anti-$p21^{ras}$ antibody. Immunoblots, quantitative densitometry for $p21^{ras}$-GTP levels, and Western blots for total $p21^{ras}$ are shown. Data are representative of five independent experiments. (B) Akt kinase activity in $Nf1^{+/-}$ and wild-type BMMCs. After preincubation with 100 nM wortmannin or DMSO control for 15 min, Akt kinase activity was determined from Akt immunoprecipitates and an in vitro kinase assay was performed using histone 2B as a phosphorylation substrate. Autoradiography and quantitative densitometry of the phosphorylation of histone 2B and Western blots for total Akt are shown. Data are representative of four independent experiments. Similar inhibition of Akt kinase was observed in cells preincubated for 15 min in 25 μM of LY294002, a second PI-3K inhibitor (data not shown).

tion of PI-3K, we performed proliferation assays with $Nf1^{+/-}$ and wild-type BMMCs in the presence or absence of the PI-3K inhibitor, LY294002. $Nf1^{+/-}$ and wild-type BMMCs were cultured in 10% fetal calf serum without growth factors for 24 h before the addition of SCF. Cell numbers were determined at the time SCF was added (day 0) and after 72 h in culture. $Nf1^{+/-}$ BMMCs showed a greater proliferative response to SCF compared with wild-type cells, as observed previously (8), and the proliferation of both mast cell genotypes was completely inhibited in the presence of LY294002 (Fig. 2 A). Similar results were obtained when mast cell proliferation was assessed using thymidine incorporation assays to measure DNA synthesis (data not shown). In addition, consistent differences in proliferation were observed between the genotypes over a range of SCF concentrations (25–100 ng/ml, data not shown). Thus, increased SCF-induced proliferation of $Nf1^{+/-}$ mast cells is mediated through hyperactivation of the $p21^{ras}$-PI-3K pathway.

While hyperactivation of the $p21^{ras}$-PI-3K signaling pathway provides a simple model to account for the phenotype of $Nf1^{+/-}$ BMMCs, we next determined which specific downstream effectors of PI-3K were responsible for the hyperproliferation of $Nf1^{+/-}$ mast cells. Recent studies in immortalized cell lines have shown that signals from PI-3K converge on the $p21^{ras}$-Raf-Mek-ERK pathway to activate ERK and promote transcription of genes that control mitogenesis (22–25). In addition, we have previously demonstrated that $Nf1^{+/-}$ BMMCs have elevated ERK activity relative to wild-type cells after stimulation with SCF which is consistent with hyperactivation of $p21^{ras}$ (8). To test whether ERK activity contributes to either wild-type or $Nf1^{+/-}$ BMMC proliferation, we performed proliferation assays as described previously with both mast cell genotypes stimulated with SCF or medium alone, in the presence or absence of the Mek inhibitor, PD98059. The Mek inhibitor completely blocked ERK activation in both mast cell genotypes after stimulation with SCF (data not shown). In multiple independent experiments ($n = 6$), addition of PD98059 reduced the proliferative response of wild-type BMMCs by ~10–15% and that of $Nf1^{+/-}$ BMMCs by 40–50% (Fig. 2 A). Importantly, whereas PD98059 caused a minimal reduction in wild-type mast cell proliferation, addition of PD98059 reduced the SCF-induced hyperproliferation of $Nf1^{+/-}$ mast cells to that of wild-type levels, establishing the importance of hyperactivation of ERK to the $Nf1^{+/-}$ proliferative phenotype (Fig. 2 A). Similar results were obtained when mast cell proliferation was assessed using thymidine incorporation assays (data not shown). Thus, these pharmacologic data suggest that hyperactivation of ERK confers a distinct proliferative advantage to $Nf1^{+/-}$ BMMCs in response to SCF.

Given that PI-3K inhibitors significantly block the proliferation of both mast cell genotypes and Mek inhibitors partially inhibit proliferation, we hypothesized that PI-3K is biochemically linked to ERK activation in BMMCs. To test this hypothesis, we stimulated both mast cell genotypes with SCF in the presence or absence of PI-3K inhibitors and measured ERK activity. Similar to previous studies (8), $Nf1^{+/-}$ BMMCs demonstrated a greater increase in ERK activity from baseline compared with wild-type cells (Fig. 2 B). However, ERK activity was completely inhibited in both genotypes in the presence of PI-3K inhibitors (Fig. 2

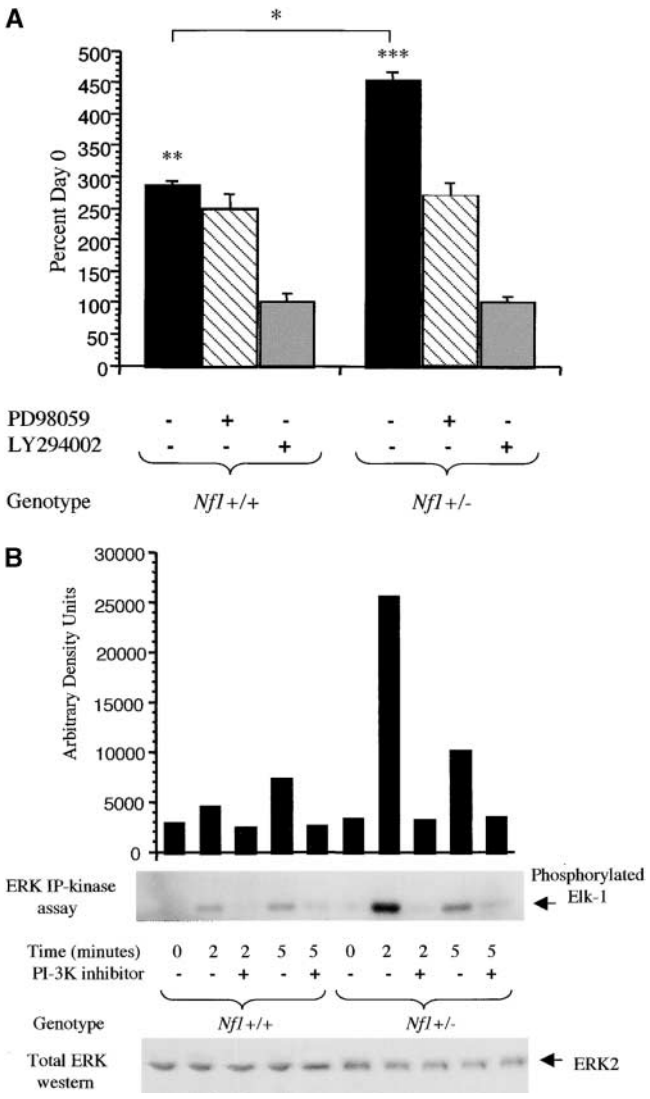

Figure 2. Effect of heterozygosity of *Nf1* on the proliferation and ERK kinase activity of BMMCs in response to SCF in the presence or absence of a Mek or PI-3K inhibitor. (A) Effect of a PI-3K or Mek inhibitor on the proliferation of $Nf1^{+/-}$ and wild-type BMMCs in response to SCF. After deprivation of growth factors for 24 h, 3×10^5 cells/ml were placed in triplicate in 24-well dishes in RPMI containing 1% glutamine, 10% fetal bovine serum, and 100 ng/ml of SCF in the presence or absence of either 50 μM PD98059 (Mek inhibitor), 10 μM LY294002 (PI-3K inhibitor), or DMSO control in a total volume of 1 ml as described previously (8). After 72 h, viable cells were counted using a hemocytometer and expressed as a percentage of input cells. $^{*}P < 0.01$ for $Nf1^{+/+}$ vs. $Nf1^{+/-}$; $^{**}P < 0.001$ for $Nf1^{+/+}$ vs. $Nf1^{+/+}$ with LY294002 or PD98059; $^{***}P < 0.01$ for $Nf1^{+/-}$ vs. $Nf1^{+/-}$ with LY294002 or PD98059 by Student's paired *t* test. (B) ERK activity in $Nf1^{+/-}$ and wild-type BMMCs after stimulation with SCF in the presence or absence of 100 nM wortmannin or DMSO control. ERK activity was determined by depriving cells of serum for 18–24 h, followed by stimulation with 10 ng/ml of SCF for 2 and 5 min. In some experiments, cells were preincubated for 15 min with 100 nM wortmannin, 25 μM LY294002 (data not shown), or DMSO control before stimulation. Autoradiography and quantitative densitometry of the phosphorylation of Elk-1 fusion protein by ERK kinase from lysates obtained from SCF-stimulated BMMCs and Western blots for total ERK are shown. Data are representative of five independent experiments.

B). Thus, these data demonstrate that ERK activation in mast cells, in response to SCF, is dependent on biochemical signals generated through PI-3K converging on the $p21^{ras}$-Raf-Mek-ERK pathway.

Cross-Cascade Activation of ERK from PI-3K Occurs at the Level of Mek and Raf-1 Kinase in $Nf1^{+/-}$ and Wild-Type Mast Cells. In other experimental systems, cross-cascade activation of ERK from PI-3K occurs at the level of either Mek or Raf-1 kinase (22–26). To test whether cross-talk between PI-3K and the $p21^{ras}$-Raf-Mek-ERK pathway occurs at the level of Mek, we stimulated $Nf1^{+/-}$ and wild-type BMMCs with SCF in the presence or absence of a PI-3K inhibitor and measured Mek activity. $Nf1^{+/-}$ BMMCs demonstrated a greater increase in Mek activity from baseline compared with wild-type cells, and Mek activity was inhibited in the presence of PI-3K inhibitors in both mast cell genotypes (Fig. 3 A).

Since Raf-1 functions as the immediate upstream effector of Mek by phosphorylating Mek Ser217/221 (27), we stimulated $Nf1^{+/-}$ and wild-type mast cells with SCF in the presence or absence of a PI-3K inhibitor and measured Raf-1 kinase activity and phosphorylation of these residues by immunoblot. Whereas wild-type BMMCs demonstrated minimal Raf-1 kinase activation after stimulation with 10 ng/ml of SCF, $Nf1^{+/-}$ BMMCs had a significant increase in Raf-1 kinase activity from baseline in multiple independent experiments ($n = 5$) which was completely inhibited in the presence of the PI-3K inhibitor (Fig. 3 B). In addition, $Nf1^{+/-}$ BMMCs had increased phosphorylation of Mek Ser217/221 which correlates with increased Raf-1 activity in these cells (Fig. 3 C). Importantly, phosphorylation of these residues was also inhibited by a PI-3K inhibitor in both mast cell genotypes (Fig. 3 C).

Taken together, as PI-3K inhibitors do not alter $p21^{ras}$ activity (data not shown), these data suggest a biochemical model where PI-3K activation of ERK occurs at the level of either Raf-1 alone or at the level of both Raf-1 and Mek in BMMCs after stimulation with SCF. Importantly, increased Raf-1 and Mek activity observed in $Nf1^{+/-}$ mast cells is consistent with the hypothesis that the hyperproliferative phenotype of $Nf1^{+/-}$ BMMCs is directly related to increased cross-talk from PI-3K to the $p21^{ras}$-Raf-Mek-ERK pathway.

Heterozygosity of Nf1 Results in Higher Basal and SCF-stimulated Rac and Pak1 Activity in BMMCs. Given the importance of cross-talk between the PI-3K and the $p21^{ras}$-Raf-Mek-ERK pathways to the hyperproliferation of $Nf1^{+/-}$ BMMCs, we performed experiments to identify proteins responsible for cross-talk between the two pathways. Studies in hematopoietic cells have positioned the small Rho GTPase, Rac, downstream of PI-3K, and some experiments in immortalized cell lines have suggested that Rac1 may function as a mediator of cross-talk between PI-3K and the $p21^{ras}$-Raf-Mek-ERK pathways (23, 28–32). Importantly, Rac1 and Rac2 activation have also been linked to mast cell proliferation but their contribution to ERK activation in mast cells has not been studied (33, 34). Given these prior experiments and our current observa-

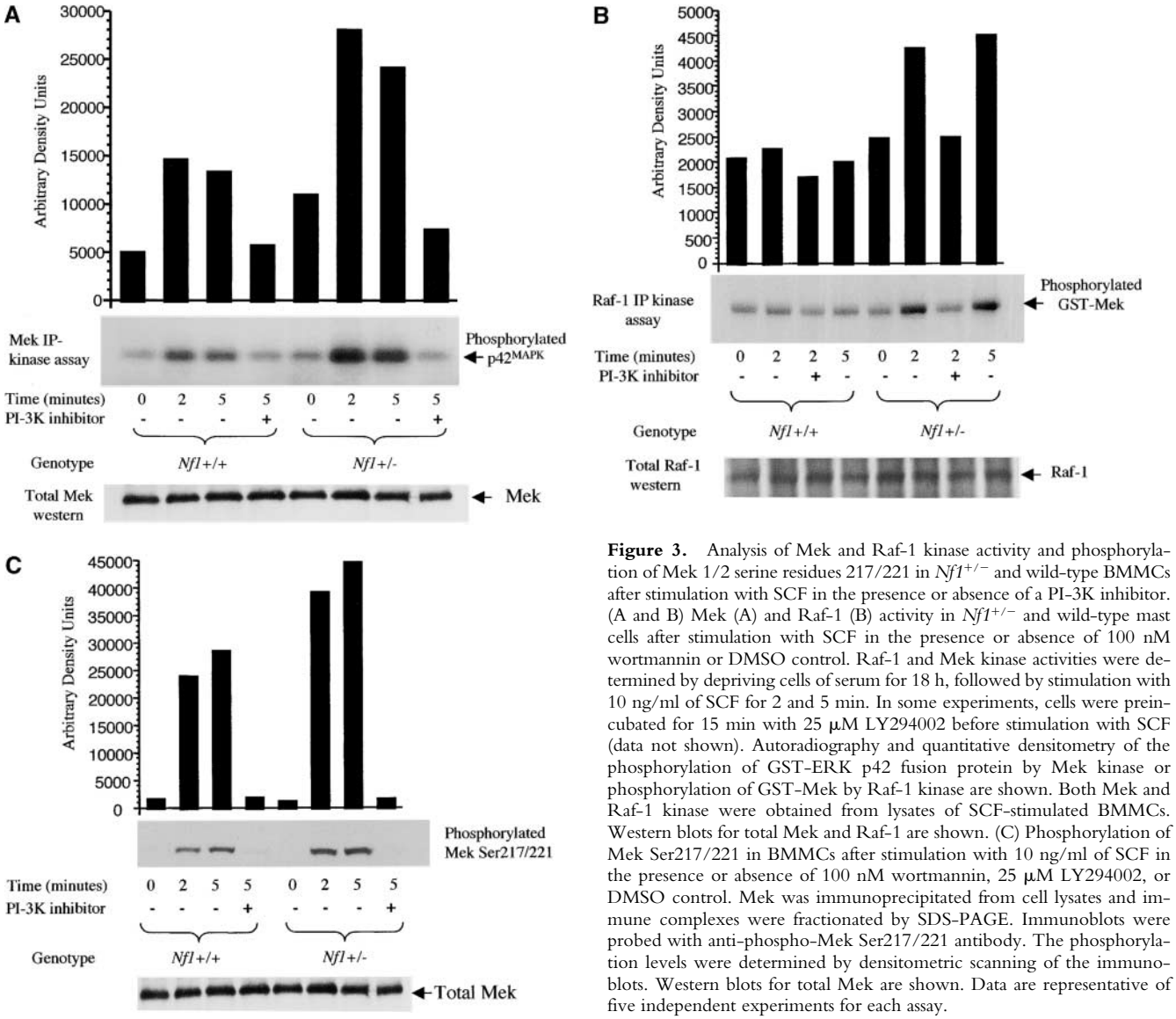

Figure 3. Analysis of Mek and Raf-1 kinase activity and phosphorylation of Mek 1/2 serine residues 217/221 in $Nf1^{+/-}$ and wild-type BMMCs after stimulation with SCF in the presence or absence of a PI-3K inhibitor. (A and B) Mek (A) and Raf-1 (B) activity in $Nf1^{+/-}$ and wild-type mast cells after stimulation with SCF in the presence or absence of 100 nM wortmannin or DMSO control. Raf-1 and Mek kinase activities were determined by depriving cells of serum for 18 h, followed by stimulation with 10 ng/ml of SCF for 2 and 5 min. In some experiments, cells were preincubated for 15 min with 25 μM LY294002 before stimulation with SCF (data not shown). Autoradiography and quantitative densitometry of the phosphorylation of GST-ERK p42 fusion protein by Mek kinase or phosphorylation of GST-Mek by Raf-1 kinase are shown. Both Mek and Raf-1 kinase were obtained from lysates of SCF-stimulated BMMCs. Western blots for total Mek and Raf-1 are shown. (C) Phosphorylation of Mek Ser217/221 in BMMCs after stimulation with 10 ng/ml of SCF in the presence or absence of 100 nM wortmannin, 25 μM LY294002, or DMSO control. Mek was immunoprecipitated from cell lysates and immune complexes were fractionated by SDS-PAGE. Immunoblots were probed with anti-phospho-Mek Ser217/221 antibody. The phosphorylation levels were determined by densitometric scanning of the immunoblots. Western blots for total Mek are shown. Data are representative of five independent experiments for each assay.

tions, we measured total Rac activity in both mast cell genotypes in response to SCF. After stimulation of BMMCs, levels of active, GTP-bound Rac in cellular lysates were determined by precipitating the active GTPase with a GST fusion of p21 activated kinase in an effector pull-down assay. $Nf1^{+/-}$ mast cells had higher basal and SCF-stimulated Rac-GTP levels compared with wild-type cells, providing evidence that $p21^{ras}$ is biochemically linked to Rac activation. (Fig. 4 A).

Pak1 is a well characterized downstream effector of Rac, and the catalytic activity of Pak1 is regulated in part by binding of Rac-GTP to the highly conserved NH_2 terminus, known as the Cdc42/Rac interactive binding (CRIB) domain (35, 36). Importantly, Pak1 has been shown to mediate cross-talk between PI-3K and the $p21^{ras}$-Raf-Mek-ERK pathway in immortalized cell lines by phosphorylating specific Raf-1 and Mek residues (22, 25). To test whether heterozygosity of *Nf1* also altered Pak1 activity in BMMCs, we measured Pak1 activity in both mast cell genotypes in response to SCF. Whereas wild-type mast cells displayed minimal Pak1 activation, $Nf1^{+/-}$ BMMCs had dramatically increased basal Pak1 activity which increased modestly after stimulation with SCF, which is consistent with increased Rac activity (Fig. 4 B). Thus, these studies suggest that hyperactivation of the Rac and potentially the Pak1 pathway confer a distinct proliferative advantage to $Nf1^{+/-}$ BMMCs.

Hyperactivation of Rac2 Directly Contributes to the Hyperproliferation and Increased ERK Activity in $Nf1^{+/-}$ BMMCs in Response to SCF. Rac2 is a hematopoietic specific Rho GTPase, and $Rac2^{-/-}$ mice have multiple mast cell defects secondary to diminished Rac activity (12, 34). Importantly, other studies have recently positioned different isoforms of Rac downstream of PI3-K in hematopoietic cells (for a review, see reference 37). To test our hypothesis that hyperactivation of Rac2 pathway is directly responsible for the

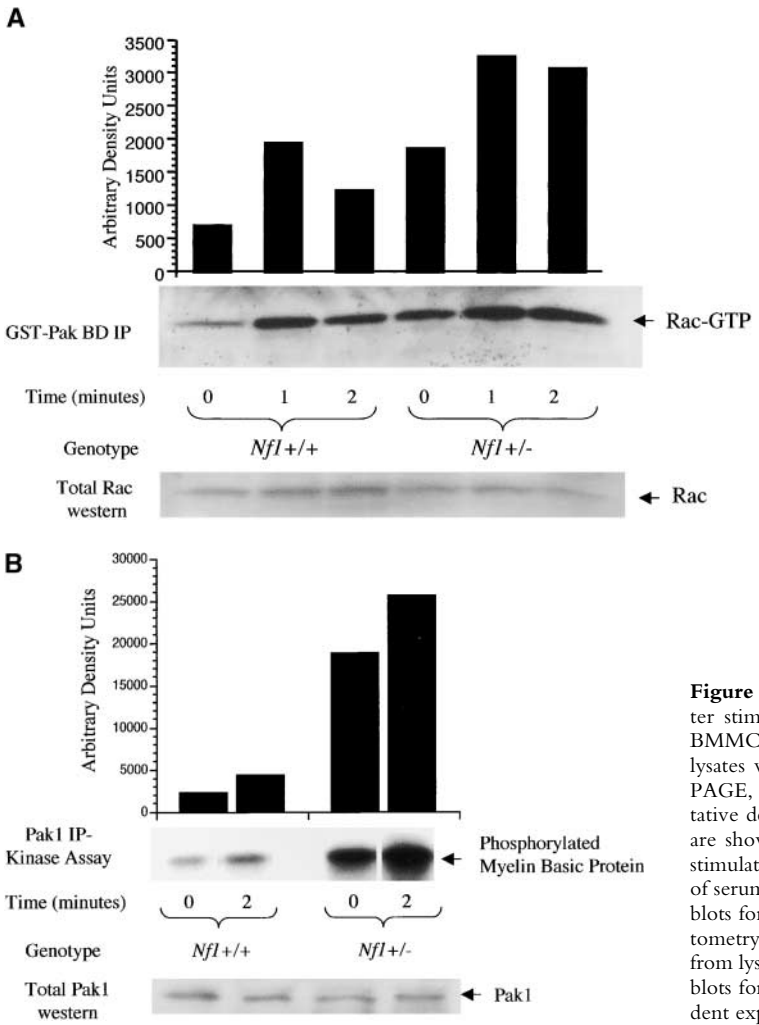

Figure 4. Effect of heterozygosity of *Nf1* on Rac and Pak1 activity after stimulation with SCF. (A) Rac activity in $Nf1^{+/-}$ and wild-type BMMCs. GTP-bound Rac levels were determined by incubating cell lysates with Pak binding domain agarose beads, fractionating by SDS-PAGE, and probing with anti-Rac antibodies. Immunoblots and quantitative densitometry for Rac-GTP levels and Western blots of total Rac are shown. (B) Pak1 activity in $Nf1^{+/-}$ and wild-type mast cells after stimulation with SCF. Pak1 activity was determined after depriving cells of serum for 18 h, followed by stimulation with SCF for 1 min. Western blots for total Pak1 are shown. Autoradiography and quantitative densitometry of the phosphorylation of myelin basic protein by Pak1 kinase from lysates obtained from SCF-stimulated BMMCs are shown. Western blots for total Pak1 are shown. Data are representative of four independent experiments for each assay.

hyperproliferation of $Nf1^{+/-}$ BMMCs and to potentially identify which Rac protein may be involved in this signaling pathway, we intercrossed $Rac2^{-/-}$ and $Nf1^{+/-}$ mice, established BMMCs from the four F2 progeny (see Materials and Methods), and performed proliferation, Pak1, and ERK activity assays. To initially determine whether Pak1 was located downstream of Rac2 in $Nf1^{+/-}$ and wild-type mast cells, BMMCs harvested from the mice of the four F2 genotypes were stimulated with SCF and Pak1 activity was measured. Consistent with our initial observations, $Nf1^{+/-}$ mast cells had higher basal and SCF induced Pak1 activity compared with wild-type cells (Fig. 5 A). However, $Nf1^{+/+}$ $Rac2^{-/-}$ and $Nf1^{+/-}Rac2^{-/-}$ BMMCs had minimal Pak1 activation at baseline and in response to SCF (Fig. 5 A). Thus, these studies identify Pak1 as a downstream effector of Rac2 in both mast cell genotypes.

To assess the role of Rac2 activation on the proliferation of $Nf1^{+/-}$ mast cells, BMMCs harvested from mice of the four F2 genotypes were cultured in 10% fetal calf serum without added growth factors for 24 h before addition of SCF. Cell numbers were determined at the time SCF was added (day 0) and after 72 h in culture. As shown previously (8, 34), $Nf1^{+/-}Rac2^{+/+}$ BMMCs showed a greater proliferative response to SCF after 72 h in culture compared with wild-type cells, whereas $Nf1^{+/+}Rac2^{-/-}$ cells showed a slight decrease in proliferation (Fig. 5 B). However, $Nf1^{+/-}Rac2^{-/-}$ BMMCs had a 40–50% reduction in proliferation compared with $Nf1^{+/-}Rac2^{+/+}$ BMMCs in response to SCF (Fig. 5 B). Importantly, the proliferative responses of $Nf1^{+/-}Rac2^{-/-}$ BMMCs were similar to wild-type cells in multiple independent experiments ($n = 6$; Fig. 5 B). Thus, these experiments provide direct genetic evidence that the hyperproliferative phenotype of $Nf1^{+/-}$ $Rac2^{+/+}$ mast cells is mediated through activation of the specific Rac2 isoform.

The reduction in proliferation of $Nf1^{+/-}Rac2^{-/-}$ BMMCs relative to $Nf1^{+/-}Rac2^{+/+}$ cells was similar to the reduction in proliferation observed with the addition of a Mek inhibitor (and subsequent inhibition of ERK activity) to the cultures of $Nf1^{+/-}Rac2^{+/+}$ mast cells. Given the similar results of these two experiments, we hypothesized that Rac2 was biochemically linked to ERK activation after stimulation of mast cells with SCF. To test this hypothesis, we compared ERK activity in the four F2 mast cell genotypes after stimulation with SCF. Consistent with prior observations, $Nf1^{+/-}Rac2^{+/+}$ mast cells had higher

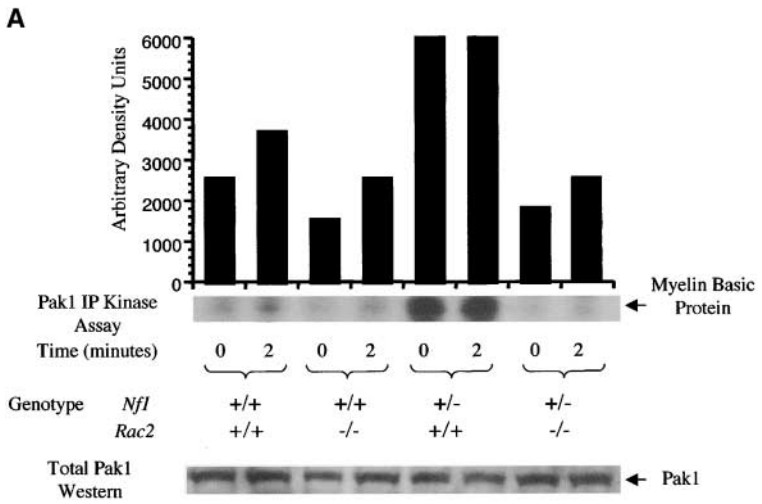

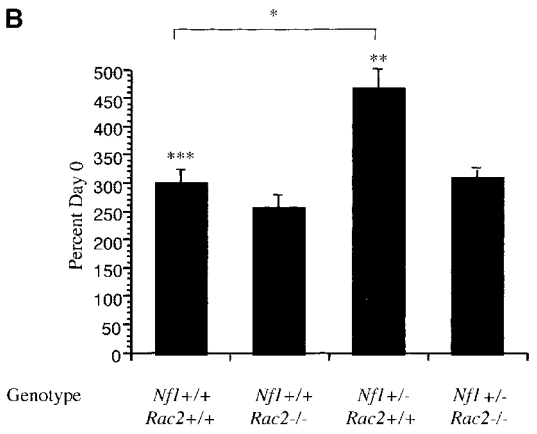

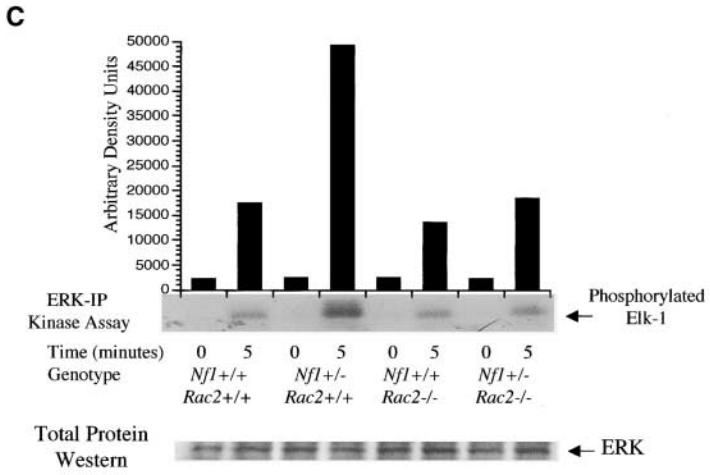

Figure 5. Effect of Rac2 deficiency on the proliferation and Pak1 and ERK kinase activity of $Nf1^{+/-}$ and wild-type BMMCs. (A) Pak1 activity in four $Nf1^{+/-}$ and $Rac2^{-/-}$ mast cell genotypes after stimulation with SCF. Pak1 activity in BMMCs harvested from the four F2 progeny composed of the following genotypes (+/+; +/+, $Nf1^{+/-}$; +/+, +/+; $Rac2^{-/-}$, $Nf1^{+/-}$; $Rac2^{-/-}$) was determined after depriving cells of serum for 18–24 h, followed by stimulation with SCF for 2 min. Autoradiography and quantitative densitometry of the phosphorylation of myelin basic protein by Pak1 kinase from lysates obtained from SCF-stimulated BMMCs and Western blots for total Pak1 are shown. (B) Proliferation of BMMCs harvested from the four F2 progeny in response to SCF. After deprivation of growth factors for 24 h, 3×10^5 cells/ml were placed in triplicate in 24-well dishes in RPMI containing 1% glutamine, 10% fetal bovine serum, and 100 ng/ml of SCF in the presence or absence of either PD98059 (Mek inhibitor), LY294002 (PI-3K inhibitor), or DMSO control in a total volume of 1 ml as described previously. After 72 h, viable cells were counted using a hemocytometer and expressed as a percentage of input cells. $^*P < 0.01$ for +/+; +/+ vs. $Nf1^{+/-}$; +/+ $^{**}P < 0.01$ for $Nf1^{+/-}$; +/+ vs. $Nf1^{+/+}$; $Rac2^{-/-}$ $^{***}P < 0.01$ for +/+; +/+ vs. $Nf1^{+/+}$; $Rac2^{-/-}$ by Student's paired *t* test. (C) Analysis of ERK activity in BMMCs stimulated with SCF in the four F2 genotypes. ERK activity was determined by depriving cells of serum for 18–24 h, followed by stimulation with 10 ng/ml of SCF for 5 min. Autoradiography and quantitative densitometry of the phosphorylation of Elk-1 fusion protein by ERK kinase from lysates obtained from SCF stimulated BMMCs and Western blots for total ERK are shown. Data are representative of five independent experiments.

ERK activity compared with wild-type cells (Fig. 5 C). However, $Nf1^{+/+}Rac2^{-/-}$ BMMCs had a 50% reduction in ERK activity compared with wild-type cells, providing genetic evidence that Rac2 is directly linked to ERK activation (Fig. 5 C). Consistent with the hypothesized role of hyperactivation of ERK to the proliferative phenotype of $Nf1^{+/-}Rac2^{+/+}$ mast cells, $Nf1^{+/-}Rac2^{-/-}$ mast cells had equivalent levels of ERK activity compared with wild-type cells in response to SCF (Fig. 5 C). Thus, these data provide further genetic confirmation that Rac2-mediated hyperactivation of ERK directly contributes to the hyperproliferation of $Nf1^{+/-}$ mast cells in response to SCF.

Increased Accumulation of Mast Cells in $Nf1^{+/-}$ Mice in Response to Local Cutaneous Administration of SCF Is Mediated through Rac2 In Vivo. Local cutaneous injection of SCF into wild-type mice results in a dramatic accumulation of mast cells at the site of injection (38, 39). Using 5-bromo-2′-deoxyuridine (Brdu) labeling in vivo, Tsai et al. demonstrated that accumulation of mast cells in this experimental model was closely linked to local cellular proliferation (39). To test whether heterozygosity at *Nf1* alters accumulation of mast cells to SCF in vivo, slow release microosmotic pumps were filled with a range of concentrations of SCF or vehicle and placed into the dorsal back skin of either wild-type or $Nf1^{+/-}$ mice. 7 d after placement, pumps were removed and cutaneous skin biopsies were taken from the site of pump insertion and stained with Giemsa stain to identify mast cells (Fig. 6, A and B). Consistent with our in vitro experiments, $Nf1^{+/-}$ mice demonstrated greater accumulation of mast cells at the site of SCF release compared with wild-type mice over a wide range of SCF doses (Fig. 6 C). Interestingly, $Nf1^{+/-}$ mice also had a greater percentage of degranulating mast cells at this dose (28 vs. 8%) compared with wild-type mice at the site of SCF release.

To investigate whether the increased accumulation of mast cells in $Nf1^{+/-}$ mice was mediated through Rac2, we repeated this experiment using the F2 progeny generated from the $Rac2^{-/-}$ and $Nf1^{+/-}$ genetic intercross. The SCF dose chosen for these experiments was 2 μg/kg/day, as the greatest difference in mast cell accumulation between wild-

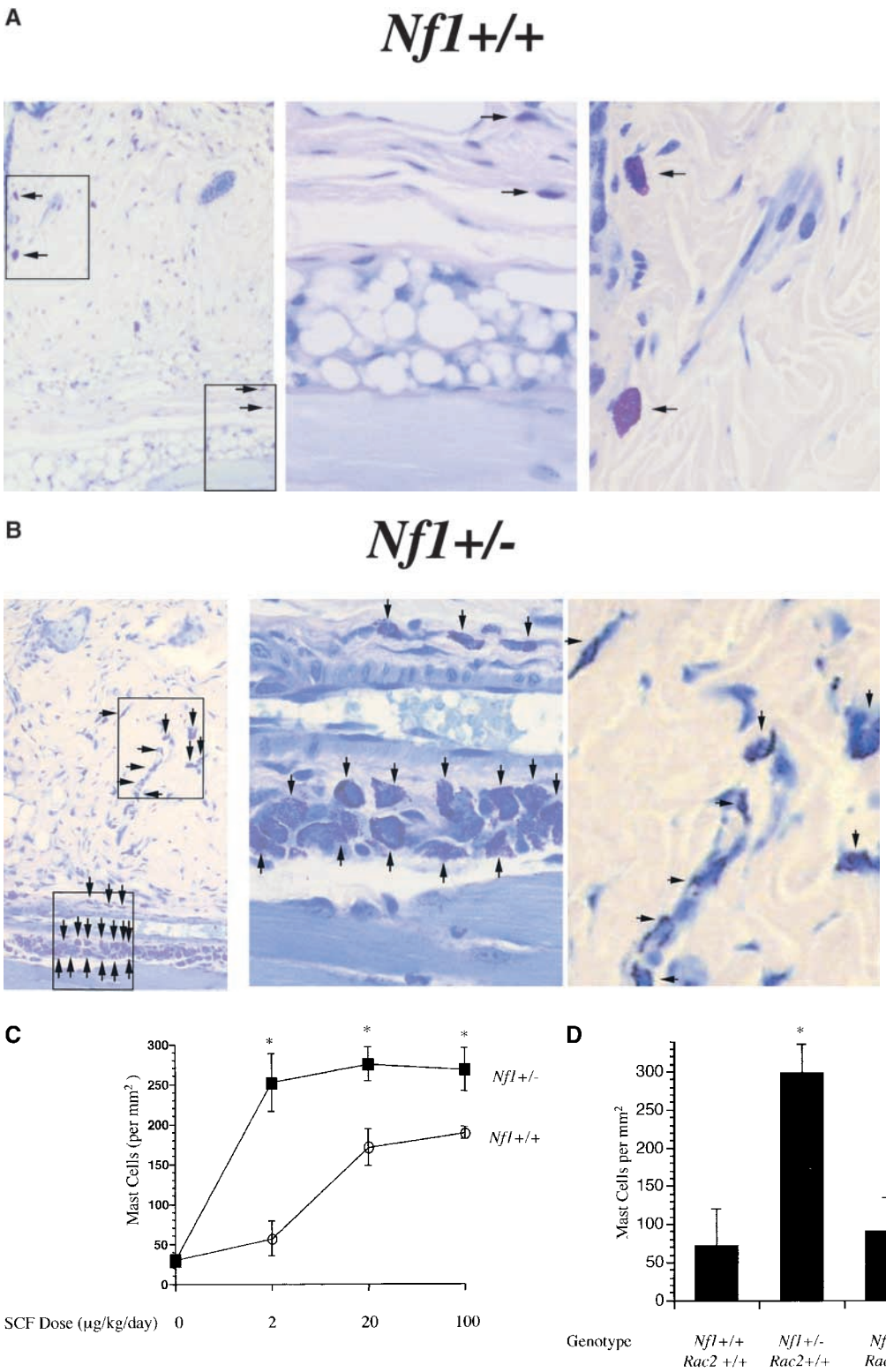

Figure 6. Effect of heterozygosity of *Nf1* on accumulation of cutaneous mast cells in response to local administration of SCF in vivo. (A and B) Representative skin biopsy stained for cutaneous mast cells taken from the site of SCF administration via a microosmotic pump on the middorsum of (A) wild-type and (B) $Nf1^{+/-}$ mice. Specimens were stained with hematoxylin and eosin to assess routine histology, and with Giemsa to identify mast cells. Cutaneous mast cells were quantitated in a blinded fashion by counting 2-mm^2 sections. A higher magnification of areas outlined in black boxes of the skin biopsy are shown to illustrate the Giemsa-positive mast cells. Black arrows indicate Giemsa-positive mast cells. (C) Number of cutaneous mast cells per mm^2 in $Nf1^{+/-}$ and wild-type mice in response to local administration of various concentrations of SCF. Osmotic pumps loaded with varying concentrations of SCF or PBS were placed subcutaneously in the dorsal skin and removed 7 d later. Specimens were processed for quantification of mast cells as described in A and B. $^*P < 0.001$ for $Nf1^{+/+}$ vs. $Nf1^{+/-}$. (D) Number of cutaneous mast cell per mm^2 in the four *Nf1* and *Rac2* genotypes. Osmotic pumps were loaded with 2 μg/kg/day of SCF or PBS, placed subcutaneously in the dorsal skin, and removed 7 d later. Specimens were processed for quantification as described above. $^*P < 0.001$ for $Nf1^{+/-}$; +/+ vs. $Nf1^{+/-}$; $Rac2^{-/-}$ by Student's paired *t* test.

type and $Nf1^{+/-}$ mice was observed at this dose (Fig. 6 C). Consistent with our in vitro proliferation results, the accumulation of mast cells in $Nf1^{+/-}Rac2^{-/-}$ mice was greatly reduced compared with $Nf1^{+/-}Rac2^{+/+}$ mice (Fig. 6 D). Importantly, no differences in mast cell accumulation were observed between wild-type and $Nf1^{+/-}Rac2^{-/-}$ mice (Fig. 6 D). To determine whether loss of Rac2 alters endogenous cutaneous mast cell numbers in $Nf1^{+/-}$ mice, histologic sections from the ears of the 4 F2 genotypes were evaluated after giemsa staining (n = 4–5 mice/group). Cutaneous sections from the ear have been found in previous studies to be a sensitive site to detect genotypic differ-

Table I. *Effects of Nf1 and Rac2 Genotypes on Cutaneous Mast Cell Numbers*

Genotype	Number of mast cells per mm^2
+/+; +/+	69 ± 4.43
Nf1$^{+/-}$; +/+	98 ± 10.32[a]
+/+; *Rac2*$^{-/-}$	63 ± 2.94[b]
Nf1$^{+/-}$; *Rac2*$^{-/-}$	63 ± 4.96[b]

Numbers of cutaneous mast cells were quantitated from ear biopsies. Results represent mean numbers of mast cells ± SEM from five animals in each genotype.
[a]$P < .053$ for comparison of *Nf1*$^{+/-}$; +/+ vs. +/+; +/+.
[b]$P < .01$ for comparison of *Nf1*$^{+/-}$; +/+ vs. +/+; *Rac2*$^{-/-}$ and *Nf1*$^{+/-}$; *Rac2*$^{-/-}$ by Student's *t* test.

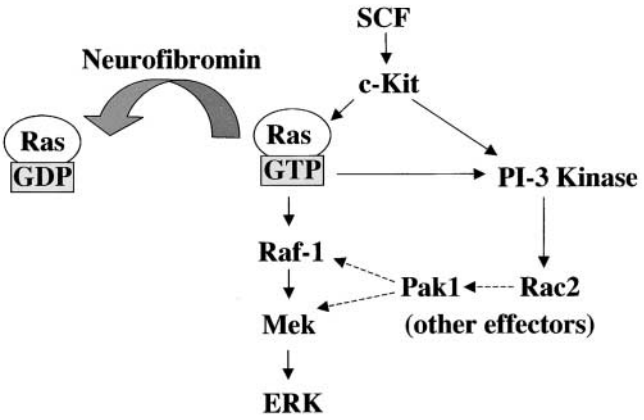

Figure 7. Schematic representation of the hypothesized biochemical pathway responsible for the hyperproliferative phenotype of *Nf1*$^{+/-}$ mast cells in response to SCF. Hatched arrows represent potential downstream effectors of Rac2.

ences in mast cell numbers (40). Interestingly, mice that were doubly mutant at *Nf1* and *Rac2* had significantly lower numbers of mast cells in the ear compared with mice that were heterozygous at *Nf1* alone (Table 1). Thus, cumulatively these studies demonstrate that the biochemical mechanisms identified in vitro for the *Nf1*$^{+/-}$*Rac2*$^{+/+}$ mast cell phenotype are operative in a more physiologic experimental system.

Discussion

Although p21^{ras} signaling outputs were originally described as operating in parallel with activation of PI-3K pathways, recent studies have suggested that receptor tyrosine kinase–mediated activation of ERK is potentially PI-3K dependent (9, 37). However, the majority of these studies were conducted in immortalized cell lines, and a clear example of the physiolgic relevance of cross-talk between the p21^{ras}-ERK and PI-3K pathways in an animal disease model has not been established previously. Multiple lineages of neurofibromin-deficient cells have a propensity to hyperproliferate in response to various growth factors which directly relates to the wide diversity of clinical manifestations observed in NF1 (41). Although neurofibromin has been shown to function as a GAP for p21^{ras} to control cellular proliferation, lack of identification of alterations in specific p21^{ras} effectors which control mitogenesis has limited our understanding of disease pathogenesis. In these experiments, we show that the hyperproliferation of *Nf1*$^{+/-}$ mast cells is directly related to increased cross-talk between the PI-3K and the p21^{ras}-Raf–ERK pathway and identify Rac2 as a principal mediator of this aberrant signaling pathway (Fig. 7).

Numerous studies have shown that active p21^{ras}-GTP can bind to multiple isoforms of the p110 catalytic subunits of type I_A PI-3K to specifically augment kinase activity (18–20). However, in neurofibromin-deficient cells, most attention has been focused on modulation of the classical p21^{ras}-Raf-Mek-ERK pathway to augment cellular proliferation. In primary mast cells, activation of PI-3K after c-kit binding to SCF is critical for controlling proliferation (15, 33). Our study shows that *Nf1*$^{+/-}$ mast cells have a twofold increase in proliferation in response to SCF compared with wild-type cells, and proliferation was completely reduced with PI-3K inhibitors, confirming the importance of PI-3K activation to the *Nf1*$^{+/-}$ cellular phenotype. Importantly, placement of cutaneous microosmotic pumps which released a continuous infusion of SCF resulted in a greater accumulation of mast cells at the site of insertion in *Nf1*$^{+/-}$ mice compared with wild-type mice. Others have previously shown that in vivo mast cell expansion in response to local injection of SCF occurs secondary to local proliferation (38, 39). Thus, our in vivo observations argue that the biochemical mechanisms identified in vitro for the *Nf1*$^{+/-}$ cell phenotype are valid and biologically operative in a more physiologic system. As *Nf1*$^{+/-}$ mast cells have increased p21^{ras} activity in response to SCF and a PI-3K inhibitor completely blocks proliferation, these cell biology studies argue that hyperactivation of the p21^{ras}-PI-3K pathway in *Nf1*$^{+/-}$ mast cells altered mast cell proliferation in vivo and in vitro.

While hyperactivation of PI-3K provides a simple model for the increased proliferation of *Nf1*$^{+/-}$ mast cells, we provide several lines of pharmacologic, genetic, and biochemical data to demonstrate that hyperactivation of the Rac2-ERK signaling pathway is directly responsible for the *Nf1*$^{+/-}$ cellular phenotype. First, we have previously reported that *Nf1*$^{+/-}$ mast cells display increased ERK activation compared with wild-type mast cells after stimulation with SCF, which is consistent with hyperactivation of p21^{ras} (8). However, we unexpectedly found that activation of ERK is dependent on signals from PI-3K and that hyperactivation of ERK was directly linked to the proliferative phenotype of *Nf1*$^{+/-}$ mast cells. PI-3K inhibitors completely blocked the activation of ERK in both mast cell genotypes. The physiological relevance of cross-talk between PI-3K and the p21^{ras}-Raf-Mek-ERK pathway in *Nf1*$^{+/-}$ cells is supported by the effect of a specific Mek inhibitor on the

SCF-stimulated proliferation of these cells. A Mek inhibitor reduces the proliferation of wild-type cells modestly (10–15%) in our studies. However, preincubation of *Nf1*$^{+/-}$ mast cells with a Mek inhibitor reduces proliferation much more significantly (40–50%), and importantly, diminishes the proliferative response to wild-type levels. Thus, in contrast to wild-type cells, hyperactivation of ERK from PI-3K provides a unique signal to confer a distinct proliferative advantage to *Nf1*$^{+/-}$ cells.

One interesting observation from these studies is that constitutive activation of multiple upstream effectors of ERK including p21^{ras} and Rac does not consistently lead to constitutive activation of ERK. One potential explanation for this observation is that mitogen-activated protein kinase phosphatase (MKP), a phosphatase that specifically binds and dephosphorylates ERK, may be elevated in *Nf1*$^{+/-}$ cells (42, 43). Recently, Brondello et al. have argued that activation of ERK regulates MKP-1 protein expression through both an increase in the rate of transcription and in the rate of proteasome-mediated degradation of MKP-1 (42, 43). Further, these authors argue that upregulation of MKP-1 in response to activation of ERK may provide an important negative feedback mechanism to limit inappropriate or constitutive activation of ERK. Given the importance of ERK activity in regulating proliferation and potentially other functions in *Nf1*$^{+/-}$ mast cells, investigation of the basal activity of this phosphatase could be important in future studies. In addition, the regulation of ERK activity in vivo is likely to be far more complex. It also remains possible that constitutive activation of upstream effectors of ERK may circumvent normal feedback mechanisms and provide a subthreshold level for activation of signaling pathways necessary for proliferation. In this context, it is intriguing to note that administration of low dosages (2 μg/kg/day) of exogenous recombinant SCF to *Nf1*$^{+/-}$ mice results in profound increases in mast cell numbers while having no significant effect on wild-type controls.

Next, given the importance of the hyperactivation of ERK to the proliferative phenotype of *Nf1*$^{+/-}$ mast cells, we focused on identifying potential mediators of cross-talk between the PI-3K and p21^{ras}-Raf-Mek-ERK pathways. Recent studies have suggested that the proliferative effects of p21^{ras} are modulated at least in part through signaling inputs from the small Rho GTPase, Rac (9). p21-activated kinase1 (Pak1) has emerged as a molecule that can link p21^{ras} and Rac signaling by converging on the p21^{ras}-Raf-Mek-ERK pathway (22, 23, 25). ERK activation has been linked to the induction of cyclin D1 expression and progression through G1 of the cell cycle (44, 45). Using a genetic intercross, we show that disruption of the hematopoietic-specific Rho GTPase, Rac2, in *Nf1*$^{+/-}$ mast cells restores the proliferative response and ERK activation of these cells to wild-type levels. Prior studies have shown that Rac1 activation of c-Jun NH2-terminal kinase (JNK) is critical for mast cell proliferation (33). However, these studies used Rac1 dominant negative constructs to transduce primary-derived mast cells, and recent data suggest that dominant negative Rac1 proteins can potentially inhibit different Rac proteins including Rac2 (46). Our genetic data demonstrate that hyperactivation of the specific Rac2 protein alters the proliferation of *Nf1*$^{+/-}$ mast cells, and provides the first evidence in primary cells that p21^{ras} and Rac2 are biochemically linked. Further, while hyperactivation of Rac2 may enhance cyclin D1 expression through increased ERK activation to promote proliferation, it is possible that Rac2 could also increase cyclin D1 accumulation through an ERK-independent mechanism. Alternatively, it is also possible that hyperactivation of the Rac2-ERK pathways promotes proliferation through a significantly different mechanism such as the transcription of genes which control autocrine production of growth factors. Though our studies cannot definitively discriminate between these possibilities, it is clear that hyperactivation of p21^{ras} and Rac2 cooperate to alter the proliferation of neurofibromin-deficient mast cells in vitro and in vivo. Studies in *Nf1*-deficient cells are currently underway to evaluate how p21^{ras} and Rac2 coordinate signals necessary for controlling cell cycle entry and progression and for measuring release of autocrine growth factors.

Using immortalized cell lines, Pak1 has been shown to increase signaling through ERK activation by phosphorylating specific residues on Raf-1 and Mek (22, 24, 25). Specifically, activated Pak1 can phosphorylate Mek1 at Ser298 to enhance the stable association between Raf-1 and Mek1 (22), and Pak1 can also phosphorylate Ser338 in the Raf-1 catalytic domain to enhance Raf-1 kinase activity (25). In these prior studies the net effect of increased activation of Mek and Raf-1 by Pak1 was increased ERK activation in response to different stimuli. Our data suggest that similar pathways are hyperactive in *Nf1*-deficient mast cells and function to increase ERK activity and proliferation in these cells. Pak1 activity and phosphorylation levels of Ser338 on Raf-1 and Ser298 on Mek1 (data not shown) in response to SCF stimulation were greatly increased in *Nf1*$^{+/-}$ mast cells compared with wild-type cells. Though our studies cannot eliminate the possibility that other effectors may contribute to cross-talk between PI-3K and the p21^{ras}-Raf-Mek-ERK pathway, our data strongly suggest that hyperactivation of the Rac2 pathway directly accounts for the hyperproliferation of mast cells (Fig. 7). The elevated levels of Pak1 activity, as well as studies where expression of a dominant negative Pak1 cDNA reduced ERK activity in *Nf1*$^{+/-}$ mast cells to wild-type levels (unpublished results), suggest that Pak1 may serve as the effector molecule of Rac2 to enhance ERK activity in Nf1$^{+/-}$ mast cells. These findings are especially intriguing, as placement of a dominant negative Pak1 or a dominant negative Rac1 has been shown to reverse the transformation of a neurofibrosarcoma cell line taken from an individual with NF1 (28). However, as dominant negative constructs may potentially bind other upstream effectors of Pak1, future studies using *Pak1* knockout mice will allow direct testing of this hypothesis. Given that different isoforms of Rac and Pak alter the biology of different neurofibromin-deficient cell lineages, further characterization of these pathways in *Nf1*$^{+/-}$ and *Nf1*$^{-/-}$ primary cells could provide insight into

the early events leading to loss of heterozygosity and the subsequent malignant manifestations in NF1.

In summary, recent studies have emphasized an increasing appreciation of the complexity of interactions between signaling pathways which control specific cellular responses. Our data provide a clear example in an animal disease model of how aberrant signaling between two major pathways can specifically alter the phenotype of a cell lineage implicated in the pathogenesis of a common genetic disease. Further characterization of this pathway and identification of similar signaling mechanisms in other neurofibromin-deficient cells should provide biochemical insight into the complex pathogenesis of NF1.

We thank Dr. Tyler Jacks for generously providing us with *Nf1* heterozygous mice. We also thank Dr. Kevin Shannon for numerous helpful scientific discussions throughout the course of these experiments and for discussions during preparation of this manuscript. Dr. David Gutmann kindly provided antisera to neurofibromin and also conducted Western blots of $Nf1^{+/-}$ mast cells. We thank Patricia Fox and Marsha Hippensteel for their help with manuscript preparation.

This work was supported by the National Institutes of Health grant R29 CA74177 (D.W. Clapp), National Institutes of Health grant R01 DK48605 (D.A. Williams), and by the National Institutes of Health Pediatric Scientist Development Program Grant K12-HD0050 (D.A. Ingram).

Submitted: 29 December 2000
Revised: 15 May 2001
Accepted: 16 May 2001

References

1. Viskochil, D., A.M. Buchberg, G. Xu, R.M. Cawthon, J. Stevens, R.K. Wolff, M. Culver, J.C. Carey, N.G. Copeland, and N.A. Jenkins. 1990. Deletions and a translocation interrupt a cloned gene at the neurofibromatosis type 1 locus. *Cell.* 62:187–192.
2. Wallace, M.R., D.A. Marchuk, L.B. Andersen, R. Letcher, H.M. Odeh, A.M. Saulino, J.W. Fountain, A. Brereton, J. Nicholson, and A.L. Mitchell. 1990. Type 1 neurofibromatosis gene: identification of a large transcript disrupted in three NF1 patients. *Science.* 249:181–186.
3. Hirota, S., S. Nomura, H. Asada, A. Ito, E. Morii, and Y. Kitamura. 1993. Possible involvement of c-kit receptor and its ligand in increase of mast cells in neurofibroma tissues. *Arch. Pathol. Lab. Med.* 117:996–999.
4. Ryan, J.J., K.A. Klein, T.J. Neuberger, J.A. Leftwich, E.H. Westin, S. Kauma, J.A. Fletcher, G.H. DeVries, and T.F. Huff. 1994. Role for the stem cell factor/KIT complex in Schwann cell neoplasia and mast cell proliferation associated with neurofibromatosis. *J. Neurosci. Res.* 37:415–432.
5. Coussens, L.M., W. Raymond, G. Bergers, M. Webster, O. Behrendtsen, Z. Werb, G. Caughey, and D. Hanahan. 1999. Inflammatory mast cells up-regulate angiogenesis during squamous epithelial carcinogenesis. *Genes Dev.* 13:1382–1397.
6. Bergers, G., R. Brekken, G. McMahon, T.H. Vu, T. Itoh, K. Tamaki, K. Tanzawa, P. Thorpe, S. Itohara, Z. Werb, and D. Hanahan. 2000. Matrix metalloproteinase-9 triggers the angiogenic switch during carcinogenesis. *Nat. Cell Biol.* 2:737–744.
7. Coussens, L.M., C.L. Tinkle, D. Hanahan, and Z. Werb. 2000. MMP-9 supplied by bone marrow-derived cells contributes to skin carcinogenesis. *Cell.* 103:481–490.
8. Ingram, D.A., F.C. Yang, J.B. Travers, M.J. Wenning, K. Hiatt, S. New, A. Hood, K. Shannon, D.A. Williams, and D.W. Clapp. 2000. Genetic and biochemical evidence that haploinsufficiency of the *Nf1* tumor suppressor gene modulates melanocyte and mast cell fates in vivo. *J. Exp. Med.* 191: 181–188.
9. Bar-Sagi, D., and A. Hall. 2000. Ras and Rho GTPases: a family reunion. *Cell.* 103:227–238.
10. DeClue, J.E., S. Heffelfinger, G. Benvenuto, B. Ling, S. Li, W. Rui, W.C. Vass, D. Viskochil, and N. Ratner. 2000. Epidermal growth factor receptor expression in neurofibromatosis type 1-related tumors and NF1 animal models. *J. Clin. Invest.* 105:1233–1241.
11. Birnbaum, R.A., A. O'Marcaigh, Z. Wardak, Y.Y. Zhang, G. Dranoff, T. Jacks, D.W. Clapp, and K.M. Shannon. 2000. Nf1 and Gmcsf interact in myeloid leukemogenesis. *Mol. Cell.* 5:189–195.
12. Roberts, A.W., C. Kim, L. Zhen, J.B. Lowe, R. Kapur, B. Petryniak, A. Spaetti, J.D. Pollock, J.B. Borneo, G.B. Bradford, et al. 1999. Deficiency of the hematopoietic cell-specific Rho family GTPase Rac2 is characterized by abnormalities in neutrophil function and host defense. *Immunity.* 10: 183–196.
13. Zhang, Y.Y., T.A. Vik, J.W. Ryder, E.F. Srour, T. Jacks, K. Shannon, and D.W. Clapp. 1998. *Nf1* regulates hematopoietic progenitor cell growth and ras signaling in response to multiple cytokines. *J. Exp. Med.* 187:1893–1902.
14. Bollag, G., D. Clapp, S. Shih, F. Adler, Y. Zhang, P. Thompson, B. Lange, M. Freedman, F. McCormick, T. Jacks, and K. Shannon. 1996. Loss of *NF1* results in activation of the Ras signaling pathway and leads to aberrant growth in hematopoietic cells. *Nat. Genet.* 12:144–148.
15. Serve, H., N. Yee, G. Stella, L. Sepp-Lorenzino, J. Tan, and P. Besmer. 1995. Differential roles of P13-kinase and kit tyrosine 821 in kit receptor-mediated proliferation, survival and cell adhesion in mast cells. *EMBO J.* 14:473–483.
16. Bollag, G., F. Adler, N. elMasry, P.C. McCabe, E. Conner, Jr., P. Thompson, F. McCormick, and K. Shannon. 1996. Biochemical characterization of a novel KRAS insertion mutation from a human leukemia. *J. Biol. Chem.* 271:32491–32494.
17. Gille, H., and J. Downward. 1999. Multiple ras effector pathways contribute to G(1) cell cycle progression. *J. Biol. Chem.* 274:22033–22040.
18. Rodriguez-Viciana, P., P. Warne, B. Vanhaesebroeck, M. Waterfield, and J. Downward. 1996. Activation of phosphoinositide 3-kinase by interaction with Ras and by point mutation. *EMBO J.* 15:2442–2451.
19. Rodriguez-Viciana, P., P.H. Warne, R. Dhand, B. Vanhaesebroeck, I. Gout, M.J. Fry, M.D. Waterfield, and J. Downward. 1994. Phosphatidylinositol-3-OH kinase as a direct target of Ras. *Nature.* 370:527–532.
20. Rodriguez-Viciana, P., P.H. Warne, A. Khwaja, B.M. Marte, D. Pappin, P. Das, M.D. Waterfield, A. Ridley, and J. Downward. 1997. Role of phosphoinositide 3-OH kinase in cell transformation and control of the actin cytoskeleton by Ras. *Cell.* 89:457–467.
21. Alessi, D.R., and P. Cohen. 1998. Mechanism of activation and function of protein kinase B. *Curr. Opin. Genet. Dev.*

8:55–62.
22. Frost, J., H. Steen, P. Shapiro, T. Lewis, N. Ahn, P. Shaw, and M. Cobb. 1997. Cross-cascade activation of ERKs and ternary complex factors by Rho family proteins. *EMBO J.* 16:6426–6438.
23. Tang, Y., J. Yu, and J. Field. 1999. Signals from the Ras, Rac, and Rho GTPases converge on the Pak protein kinase in Rat-1 fibroblasts. *Mol. Cell. Biol.* 19:1881–1891.
24. Sun, H., A.J. King, H.B. Diaz, and M.S. Marshall. 2000. Regulation of the protein kinase Raf-1 by oncogenic Ras through phosphatidylinositol 3-kinase, Cdc42/Rac and Pak. *Curr. Biol.* 10:281–284.
25. Chaudhary, A., W.G. King, M.D. Mattaliano, J.A. Frost, B. Diaz, D.K. Morrison, M.H. Cobb, M.S. Marshall, and J.S. Brugge. 2000. Phosphatidylinositol 3-kinase regulates raf1 through pak phosphorylation of serine 338. *Curr. Biol.* 10: 551–554.
26. Garrington, T., and G. Johnson. 1999. Organization and regulation of mitogen-activated protein kinase signaling pathways. *Curr. Opin. Cell Biol.* 11:211–218.
27. Alessi, D.R., Y. Saito, D.G. Campbell, P. Cohen, G. Sithanandam, U. Rapp, A. Ashworth, C.J. Marshall, and S. Cowley. 1994. Identification of the sites in MAP kinase kinase-1 phosphorylated by p74raf-1. *EMBO J.* 13:1610–1619.
28. Tang, Y., S. Marwaha, J.L. Rutkowski, G.I. Tennekoon, P.C. Phillips, and J. Field. 1998. A role for Pak protein kinases in Schwann cell transformation. *Proc. Natl. Acad. Sci. USA.* 95:5139–5144.
29. Wennstrom, S., P. Hawkins, F. Cooke, K. Hara, K. Yonezawa, M. Kasuga, T. Jackson, L. Claesson-Welsh, and L. Stephens. 1994. Activation of phosphoinositide 3-kinase is required for PDGF-stimulated membrane ruffling. *Curr. Biol.* 4:385–393.
30. Wennstrom, S., A. Siegbahn, K. Yokote, A.K. Arvidsson, C.H. Heldin, S. Mori, and L. Claesson-Welsh. 1994. Membrane ruffling and chemotaxis transduced by the PDGF beta-receptor require the binding site for phosphatidylinositol 3′ kinase. *Oncogene.* 9:651–660.
31. Ma, A.D., A. Metjian, S. Bagrodia, S. Taylor, and C.S. Abrams. 1998. Cytoskeletal reorganization by G protein-coupled receptors is dependent on phosphoinositide 3-kinase gamma, a Rac guanosine exchange factor, and Rac. *Mol. Cell. Biol.* 18:4744–4751.
32. Han, J., K. Luby-Phelps, B. Das, X. Shu, Y. Xia, R.D. Mosteller, U.M. Krishna, J.R. Falck, M.A. White, and D. Broek. 1998. Role of substrates and products of PI 3-kinase in regulating activation of Rac-related guanosine triphosphatases by Vav. *Science.* 279:558–560.
33. Timokhina, I., H. Kissel, G. Stella, and P. Besmer. 1998. Kit signaling through PI 3-kinase and Src kinase pathways: an essential role for Rac1 and JNK activation in mast cell proliferation. *EMBO J.* 17:6250–6262.
34. Yang, F.-C., R. Kapur, A.J. King, W. Tao, C. Kim, J. Borneo, R. Breese, M. Marshall, M.C. Dinauer, and D.A. Williams. 2000. Rac2 stimulates Akt activation affecting BAD/Bcl-XL expression while mediating survival and actin function in primary mast cells. *Immunity.* 12:557–568.
35. Bagrodia, S., and R.A. Cerione. 1999. Pak to the future. *Trends Cell Biol.* 9:350–355.
36. Daniels, R.H., and G.M. Bokoch. 1999. p21-activated protein kinase: a crucial component of morphological signaling? *Trends Biochem. Sci.* 24:350–355.
37. Stephens, L., A. McGregor, and P. Hawkins. 2000. Phosphoinositide 3-kinases: regulation by cell-surface receptors and function of 3-phosphorylated lipids. *In* Biology of Phosphoinositides. S. Cockcroft, editor. Oxford University Press, New York. 32–108.
38. Iemura, A., M. Tsai, A. Ando, B. Wershil, and S. Galli. 1994. The c-kit ligand, stem cell factor, promotes mast cell survival by suppressing apoptosis. *Am. J. Pathol.* 144:321–328.
39. Tsai, M., L. Shih, G. Newlands, T. Takeishi, K. Langley, K. Zsebo, H. Miller, E. Geissler, and S. Galli. 1991. Rat c-kit ligand, stem cell factor, induces the development of connective tissue-type and mucosal mast cells in vivo. Analysis by anatomical distribution, histochemistry, and protease phenotype. *J. Exp. Med.* 174:125–131.
40. Lorenz, U., A.D. Bergemann, H.N. Steinberg, J.G. Flanagan, X. Li, S.J. Galli, and B.G. Neel. 1996. Genetic analysis reveals cell type-specific regulation of receptor tyrosine kinase c-Kit by the protein tyrosine phosphatase SHP1. *J. Exp. Med.* 184:1111–1126.
41. Friedman, J., D. Gutmann, M. MacCollin, and V. Riccardi. 1999. Neurofibromatosis: Phenotype, Natural History and Pathogenesis. 3rd ed. The Johns Hopkins University Press, Baltimore, MD. 381 pp.
42. Brondello, J.M., J. Pouyssegur, and F.R. McKenzie. 1999. Reduced MAP kinase phosphatase-1 degradation after p42/p44MAPK-dependent phosphorylation. *Science.* 286:2514–2517.
43. Brondello, J.M., A. Brunet, J. Pouyssegur, and F.R. McKenzie. 1997. The dual specificity mitogen-activated protein kinase phosphatase-1 and -2 are induced by the p42/p44MAPK cascade. *J. Biol. Chem.* 272:1368–1376.
44. Cheng, M., V. Sexl, C. Sherr, and M. Roussel. 1998. Assembly of cyclin D-dependent kinase and titration of p27Kip1 regulated by mitogen-activated protein kinase kinase (MEK1). *Proc. Natl. Acad. Sci. USA.* 95:1091–1096.
45. Kerkhoff, E., and U. Rapp. 1998. Cell cycle targets of Ras/Raf signalling. *Oncogene.* 17:1457–1462.
46. Gu, Y., B. Jia, F.-C. Yang, M. D'Souza, C.E. Harris, C.W. Derrow, Y. Zheng, and D.A. Williams. 2001. Biochemical and biological characterization of a human Rac2 GTPase mutant associated with phagocytic immunodeficiency. *J. Biol. Chem.* 276:15929–15938.